Distribution Agreement

In presenting this thesis as a partial fulfillment of the requirements for a degree from Emory University, I hereby grant to Emory University and its agents the non-exclusive license to archive, make accessible, and display my thesis in whole or in part in all forms of media, now or hereafter now, including display on the World Wide Web. I understand that I may select some access restrictions as part of the online submission of this thesis. I retain all ownership rights to the copyright of the thesis. I also retain the right to use in future works (such as articles or books) all or part of this thesis.

Lindsay Fogel November 30, 2021

ATF4-Controlled BECN1 Vectors for Treatment of Huntington's Disease in R6/2 Mice

by

Lindsay Fogel

Claire-Anne Gutekunst, PhD.

Adviser

Neuroscience and Behavioral Biology

Claire-Anne Gutekunst

Adviser

John Heemstra, Jr.

Committee Member

Joseph Manns

Committee Member

2021

ATF4-Controlled BECN1 Vectors for Treatment of Huntington's Disease in R6/2 Mice

By

Lindsay Fogel

Claire-Anne Gutekunst, PhD.

Adviser

An abstract of
a thesis submitted to the Faculty of Emory College of Arts and Sciences
of Emory University in partial fulfillment
of the requirements of the degree of
Bachelor of Science with Honors

Neuroscience and Behavioral Biology

2021

Abstract

ATF4-Controlled BECN1 Vectors for Treatment of Huntington's Disease in R6/2 Mice

By Lindsay Fogel

Background: Huntington's disease (HD) is a rare genetic neurodegenerative disorder that affects approximately 2.7 people per 100,000 worldwide. The disease is characterized by a variety of motor, psychiatric, and cognitive symptoms before its ultimately fatal course. Currently, there are no therapeutic options capable of slowing or halting disease progression. Accumulation of mutant huntingtin protein has been found to activate the unfolded protein response (UPR) and contribute to endoplasmic reticulum (ER) stress, resulting in downstream effects implicated in disease progression. However, one novel therapeutic strategy that capitalizes on this dysregulation is the regulation of protein clearance via BECN1 in response to indicators of intracellular stress. Activating transcription factor 4 (ATF4) is translated according to the PERK signaling pathway in the UPR and can serve as an indicator of intracellular stress. As such, expression of BECN1 in response to translation of ATF4 represents an opportunity to modulate the delivery of BECN1 to enhance neuroprotection and halt disease progression.

Methods: R6/2 mice received bilateral striatal injections of AAV2-derived therapies (ATF4-GFP, ATF4-BECN1, GFP, BECN1) and underwent a series of behavioral assessments to measure motor skills, including climbing tests, as well as weekly weigh-ins as an indicator of disease progression. Following completion, post-mortem neuropathological assessments were conducted to understand the extent of vector spread and reduction of htt aggregates.

Results: With regard to behavioral skills, including climbing, rearing, and movement on the mesh, the treatment did not have a significant effect on motor decline and progression. There was not a significant difference in weekly weights among the treatment groups for Huntington's mice. However, upon neuropathological analysis of ATF4-GFP and ATF4-BECN1 groups, ATF4-BECN1 mice on average had fewer htt aggregates present within striatal sections where the treatment was present.

Conclusion: While the gene therapy did not significantly alter motor skills in R6/2 mice, the decreased presence of htt aggregates suggests the therapy could be improved and offer potential for therapeutic regulation. Possible improvements include increased vector spread through the use of a different AAV serotype, as well as testing in an HD model with a slower rate of disease progression than the R6/2 model.

ATF4-Controlled BECN1 Vectors for Treatment of Huntington's Disease in R6/2 Mice

By

Lindsay Fogel

Claire-Anne Gutekunst

Adviser

A thesis submitted to the Faculty of Emory College of Arts and Sciences
of Emory University in partial fulfillment
of the requirements of the degree of
Bachelor of Science with Honors

Neuroscience and Behavioral Biology

2021

Acknowledgements

I would like to thank Dr. Claire-Anne Gutekunst and Dr. Gross for allowing me to conduct research in their laboratories at Emory University. I would also like to thank the following members of the Gross Laboratory at Emory University: Dr. Alejandra Fernandez and Dr. Angel Santiago-Lopez. I would like to give special recognition to Dr. Angel Santiago-Lopez for his incredible mentorship and assistance developing my thesis proposal, as well as Dr. Claire-Anne Gutekunst for her expertise, time, and knowledge throughout the completion of my thesis. Finally, I would like to thank my father, Dr. Robert Fogel, my mother, Joann Fogel, and my sister, Olivia Fogel, for their support.

Table of Contents

Figures

Introduction

Huntington's disease (HD) is a rare, progressive, neurodegenerative disorder estimated to affect 2.7 people per 100,000 worldwide, with the highest rates among Western populations[1]. HD is an autosomal dominant disorder characterized by motor deficits, psychiatric symptoms, and cognitive abnormalities, with disease onset typically around 45 years of age, although a small percentage of individuals develop juvenile HD, which manifests earlier[2]. While symptoms can vary considerably, the condition is characterized by motor deficits, psychiatric symptoms, and cognitive abnormalities that progressively worsen during the ultimately fatal course of the disease. Motor symptoms include choreiform movements during the early phase of the disease, with bradykinesia, rigidity, and parkinsonian-like symptoms during late stages. Cognitive decline may be detected years before other symptoms and may include decreases in attention and mental flexibility[3]. Psychiatric symptoms vary, but range from depression to irritability and impulsivity[3]. Following development of manifest HD, affected individuals survive 15-18 years on average as the disease progresses and enhances biological aging processes[2]. The approximate 50% risk for offspring of those who carry the gene, along with the uniformly progressive and ultimately fatal course of the disease, underscore the clear need for novel therapies to slow/halt this progression.

Although HD was first identified and described in the late 1800s, the mutation responsible in the huntingtin gene (HTT) was discovered over 100 years later in 1993. The mutated gene includes an expansion of the CAG trinucleotide repeat, with repeats exceeding 35 contributing to the disease state. As a result, a mutated form of the huntingtin protein (mHTT) is translated with an

elongated polyglutamine tract. The exact mechanism by which mHTT drives pathogenesis is still under investigation, but the diseased brain is characterized by dysfunction and cell loss in the striatum, among other areas. Misfolded mHTT is thought to maintain a toxic gain-of-function as compared to the wild-type huntingtin (wtHTT) protein, disrupting normal function, and driving dysregulation and neurodegeneration[1]. Additionally, the mutant protein aggregates within many areas of the brain and other peripheral organs, possibly leading downstream to the multitude of symptoms associated with HD. Identification of specific areas of neuronal loss and thinning, as well as identification of mHTT, has given rise to the development of numerous toxin-based and genetic-based models of HD. Through these models, several potential therapies have been studied and continue to be examined given the lack of treatments available to delay onset or halt progression, including therapies targeting mHTT clearance.

Neuropathology, biology, and genetic factors related to HD

While George Huntington first described HD in 1872, the autosomal dominant genetic mutation in the huntingtin (HTT) gene responsible for disease onset was not discovered until a century later in 1993[3]. As a result, identification of physiological and symptomatic hallmarks preceded understanding of the neuropathological mechanisms underlying the disease. The responsible gene encodes for the 3,144-amino acid long HTT protein[3], which is well-conserved in several species ranging from flies to mammals[4]. The genetic basis of the disease state in humans is characterized by an extended polyglutamine stretch due to abnormal CAG repeats in the N-terminal sequence, contributing to protein misfolding and aggregation. Several components of disease pathology have been the focus of many studies, including understanding cell death in HD,

elucidating the natural function of the huntingtin protein, examining proteostasis and the stress response, and impaired protein clearance mechanisms.

Neuronal loss and degeneration

Progressive loss of neuronal function has been attributed to brain region atrophy and premature neuronal death in several brain structures, with the most prominent degeneration occurring in the basal ganglia[5]. The best-characterized neuropathological feature is the reduction in size of the neostriatum due to gross atrophy of the caudate nucleus and putamen[6–8]. The dramatic neostriatal neuron loss is mainly due to degeneration of medium spiny GABAergic projection neurons, which are the terminals of striatal projection neurons and serve as the main efferent output[9]. Striatal atrophy is thought to underly an array of key motor and cognitive deficits associated with HD, ranging from chorea and dystonia to disordered planning and impulsive behavior[9,10].

Function of the HTT protein

The differences between the wild-type (wHTT) and mutant protein (mHTT) may alter several roles of wHTT, including its mechanisms pertaining to transcriptional regulation, brain-derived neurotrophic factor (BDNF) production, axonal transport, vesicular recycling, and organelle trafficking[11–13]. As such, mHTT toxicity is thought to be related to interference with the above pathways. In addition, there is data to suggest toxic gain-of-function roles of mHTT that affects numerous downstream pathways, such as: early transcriptional dysregulation, synaptic dysfunction, altered axonal trafficking, impairment of the proteostasis network, excitotoxicity,

mitochondrial dysfunction, and aggregate pathology[14–16]. Therapeutic efforts to directly target these downstream pathways have been unsuccessful thus far[17], suggesting that the root cause of disease must be addressed to achieve clinical improvements.

ER stress and the UPR

A promising approach for addressing early steps in HD dysfunction resides in targeting stress responses, protein homeostasis (proteostasis), and quality control mechanisms. The proteostasis network regulates protein synthesis, folding, and degradation. Failure in the network, including impaired folding or protein clearance, can lead to protein aggregation and activation of the unfolded protein response (UPR) or heat shock response[18,19]. Additionally, data from HD models suggests that accumulation of mHTT is associated with dysfunctional proteostasis, including an inability to clear misfolded mHTT aggregates[20,21]. While the exact mechanisms through which mHTT contributes to neuropathology are unknown, aggregation of the misfolded protein is deeply intertwined with inducing intracellular stress through the endoplasmic reticulum (ER)[22]. For example, Reijonen et al. showed that inhibiting ER stress counteracted apoptosis and aggregation induced by mHTT by influencing calcium metabolism and activating signaling proteins Chop, JNK, and c-jun found downstream in the inositol-requiring enzyme 1 (IRE1) and PKRK-like ER kinase (PERK) pathways[23,24].

The unfolded protein response (UPR) represents a potential pathway that contributes to neuronal loss in HD following ER-induced activation. ER stress due to the accumulation of misfolded mHTT activates the UPR, contributing to an upregulation in transcription of

chaperone proteins, activation of protein degradation through proteasome systems, and modulating translation[22]. However, chronic ER stress and persistent UPR activation can induce neuronal apoptosis, which has the potential to contribute to the cell death and atrophy present in HD [22]. Another important finding revealed that expression of UPR genes in the striatum correlates with the number of CAG repeats in mice models of HD, potentially involving this mechanism in juvenile and early-onset disease in humans [22]. Protein kinase RNA-like ER kinase (PERK) serves as one of the signaling pathways driving the UPR and contributes to a decrease in protein translation by phosphorylating the eukaryotic initiation factor 2a (eIF2a)[25]. The phosphorylation state of eIF2a directly contributes to the translation of activating transcription factor 4 (ATF4) such that eIF2a is connected to the selective translation of ATF4 and can thereby serve as an indicator of cellular stress [26,27]. These intracellular sensors can detect stress and therefore serve as a guide to enable protein quality control in a regulated fashion.

Increasing evidence suggests that ER stress is a significant factor in cellular degeneration and can be generated by misfolded proteins, subsequently triggering activation of the UPR[28]. UPR pathways rely on activation of various ER transmembrane proteins that are inactive under normal conditions: PERK, IRE1, and activating transcription factor 6 (ATF6)[29]. Upon activation, PERK phosphorylates eukaryotic translation initiation factor 2a (eIF2a), which halts the initiation of protein translation to reduce subsequent protein synthesis[30]. However, other proteins, such as ATF4, are preferentially translated, which activates genes related to protein folding, nutrient metabolism, and apoptosis under severe stress by induction of CHOP/GADD153[31–34].

Although the direct connection between HD and the UPR is unclear, there are several theories as to how mHTT induces the ER stress response. For example, evidence from HD cellular models indicates that cytosolic mHTT fragments impair ER-associated protein degradation (ERAD) due to the entrapment of essential ERAD proteins, including Npl4, Ufd1, and p97[35]. As a result, the normal function of this protein complex, which involves facilitating the transport of ERAD substrates from the ER to the cytosol and proteasome, is inhibited[35,36]. Additionally, another possible route of ER stress induction is via disruption of ER/Golgi vesicular trafficking, thereby resulting in either ER calcium homeostasis disturbance or protein overload[37]. Despite insufficient understanding of the exact mechanism of UPR activation in HD, experimental data has indicated that the expression of UPR genes tends to negatively correlate with the number of CAG repeats in the striatum in mice models of the disease[22]. The observed relationship between the length of polyglutamine tracts in mice and UPR gene expression suggests these pathways may contribute to disease pathology and progression[22].

Disrupted protein quality control

Disruptions to protein homeostasis (proteostasis) contribute to the accumulation of misfolded proteins, often attributed to impaired degradative pathways, impaired molecular chaperones, or inadequacies in conformational stability of proteins. Intracellular organelles and proteins are regulated by one of two primary quality control mechanisms: the ubiquitin proteasome system (UPS) and the autophagy-lysosomal (autophagy) system. Each system has an important role in recycling or removing damaged or malfunctioning cellular components when repair is not possible. Disruption of proteostasis can result in the post-translation ubiquitylation of proteins,

enabling recognition by systems for degradation[38]. Although pathogenic forms of HTT may be labelled utilizing ubiquitin and thus potentially represent substrates for degradation, UPS activity is suspected to be reduced in HD, but conflicting evidence prevents definitive conclusions[39]. For example, Wang et al. targeted fluorescent reporters for the UPS in a mouse model of HD, demonstrating a decrease in synaptic UPS activity for both cultured neurons and in HD R6/2 mouse brains that expressed mHTT[40]. However, further studies examining the role of the UPS in the presence of mHTT-derived inclusion bodies from Tet/HD94 mouse models did not show significant changes in activity, contributing to an unclear interaction between mHTT and the UPS[41]. Differences in model phenotypes and genotypes may, in part, explain the inconsistent results.

With regard to the autophagy pathway for degradation, wHTT modulates autophagy function in a neuroprotective manner and the mutant form can induce toxicity due to defective pathways[42]. Mutant huntingtin has been found to interfere with cargo recognition and reduce autophagosome motility, enhancing the ability of mHTT to accumulate without normal removal mechanisms[43,44]. Moreover, in vitro and preclinical studies reveal that pharmacologically modulating autophagy can not only reduce protein aggregation and disease burden, but also minimize neuronal degeneration[45–47] Despite proposed interference with autophagocytotic mechanisms in the presence of mHTT, abnormalities were reported in models of huntingtin depletion as well, suggesting a physiological role for the wild-type protein in normal autophagy induction[48,49]. The potential functional role of wHTT in macroautophagy induction, along with

toxic effects due to mHTT, serve as a basis for enhancing understanding of autophagic impairments in HD that hinder aggregate clearance.

Molecular chaperones aid in the normal folding activity of proteins and have been implicated in HD through reductions in the level of different chaperones, as identified in HD mice[50,51], and through hinderances due to mHTT. mHTT competes with other proteins for chaperone binding[52] and sequesters chaperones in its aggregates[53,54], thereby reducing chaperone availability. Additionally, heat shock factor 1 (Hsf1), one of the primary mediator of transcriptional responses to deviation from protein homeostasis, are decreased in human HD brains, offering insight into another mechanism of pathogenesis due to the role of Hsf1 in activating the heat shock response[51,55]. Several modulatory approaches targeting chaperone function have been proposed to mediate mHTT aggregation and accumulation, including inhibition of heat shock protein (Hsp) 90 to drive mHTT degradation through activation of UPS[56] or by eliciting the heat shock response[57]. Due to the dual role of molecular chaperones in proper protein folding and mediating autophagy to enhance degradation, this proteostasis network component represents an additional avenue for modulating protein quality control. The cellular changes above are directly responsible for the pathology seen, including significant striatal atrophy and neurodegeneration. Ultimately, the neurophysiological abnormalities driven by the underlying mechanisms associated with the presence of the mutant protein and its oligomeric aggregates contributes to key clinical features, ranging from choreic movement and psychiatric disturbances to enhanced biological aging and ultimately premature death.

Resolving disrupted protein quality control

In normal neuronal cells, there are two primary pathways for protein quality control: the ubiquitin-proteasome system and the autophagy-lysosomal pathway (autophagy). Each system maintains an important role in destruction and recycling of altered components of the cell when repair is not possible[58]. Autophagy represents an evolutionary conserved mechanism of degradation but has been identified as defective in several neurodegenerative disorders, including HD[49]. Furthermore, mutant huntingtin has been found to interfere with cargo recognition and decrease autophagosome motility, enhancing the ability of mHTT to accumulate without normal removal mechanisms[59]. Moreover, in vitro and preclinical studies reveal that pharmacologically modulating autophagy can not only reduce protein aggregation and disease burden, but also minimize neuronal degeneration[60].

BECN1 is an autophagy-inducing gene found to have an age-dependent decline in human brains[61]. In addition to decreased levels of BECN1 throughout the aging process, decreased levels and sequestration of BECN1 has been reported in HD brains[62]. Overexpression of BECN1 in primary neuronal culture HD models has shown neuroprotective effects[63], suggesting its expression can drive mHTT protein clearance and provide an opportunity to remove the aggregates worsening disease pathology[61]. Given the role of BECN1 in regulating intracellular levels of mHTT and the reduction of the BECN1-regulated autophagy pathway in HD, an emerging therapeutic strategy for modulating autophagy involves activating BECN1. Attenuating the activation of BECN1 in response to the detected level of disease state as indicated by ATF4 levels

and the UPR has the potential to drive downstream effects of mHTT clearance in a self-regulated loop, minimizing possible negative implications.

Hypothesis

By utilizing a gene therapy in vivo where the autophagy inducer BECN1 is expressed in response to translation of activating transcription factor 4 (ATF4), we will be able to detect intracellular stress associated with misfolded mutant htt and modulate the delivery of BECN1 accordingly in a regulated manner to enhance neuroprotection and halt disease progression.

Methods

To test the above hypothesis, we utilized a combination of behavioral assessments and neuropathological assessments. R6/2 male mice (N=4 to 6 per viral vector) were injected with either cGFP, cBECN1, ATF4-GFP, or ATF4-BECN1 at 4 weeks of age. The R6/2 mouse model was developed following the discovery of the mutant huntingtin gene in 1993 and advancements in molecular technology, enabling the introduction of genes into rodents' germlines to express mHTT[64]. The first transgenic mouse models developed, R6/1 and R6/2, remain the most commonly used models, involving random insertion of the human gene containing the CAG repeat with expression driven by various promoters[64]. The R6/2 model is created by inserting a 1.9-kB fragment from the 5' end of the mutant human htt gene into the mouse's genome[65]. The fragment, which only contains exon 1 from the human gene, expresses 144 CAG repeats with mutant htt expression driven by the human HTT promoter[65]. These mice display an array of motor symptoms, including: involuntary jerks that resemble chorea; stereotypic involuntary

movements, such as repetitive stroking of the nose and a hind limb kicking motion; clasping behavior; weight loss; and epileptic seizures[65].

The AAV-based vectors represent either treatment or control groups based on the presence or absence of ATF4 and/or BECN1. Given that ATF4 is selectively translated during proteostasis dysregulation, upon recognition of htt aggregation, ATF4 should be translated and thus drive the expression of autophagy inducer BECN1. The mice received injections of the viral vectors bilaterally into the striatum given that striatal atrophy and mutant htt accumulation occurs during pathogenesis. Behavioral assessments, including a climbing test and a clasping test performed in R6/2 transgenic mice, were utilized to examine the efficacy of ATF4-controlled BECN1 expression by examining changes in behavior over time. For neuropathological assessments, we used a combination of staining and immunofluorescence to visualize the protein vectors and capture images via microscopy. Additionally, we measured mice body weight several times a week as another indicator of disease progression. A total of 27 R6/2 mice from The Jackson Laboratory and 5 wild-type mice were included in the study for comparison purposes across the different treatment groups.

Behavioral Assessments

The effect of ATF4-BECN1 on body weight, climbing skills, and clasping, were explored and compared to mice injected with either cGFP, cBECN1, or ATF4-GFP using a 2-way ANOVA statistical analysis. Throughout the scoring process, the treatment groups were unknown and blinded to scorers. Results were analyzed and graphed via Prism software.

Climbing test

This assay was implemented beginning one-week post-injections and involved examining climbing behavior in a wire-mesh cage. For the climbing test, mice were placed in the center of a cage for a 10-minute period. The video-tapings were reviewed thereafter in a blinded fashion to analyze the number of times each mouse climbed onto the wire mesh. Rearing behavior was counted and analyzed as well, along with tracking of the amount of time each mouse spent on the wire mesh during each climb compared to the amount of time spent at the bottom of the chamber. The climbing assay was performed weekly to track changes in behavior as the disease progressed. These tests were videotaped for review and scoring over the course of several weeks.

Neuropathological Assessment

Approximately 8 weeks post-surgery (or when mice were not able to right themselves after 30s when placed on their sides), mice were sacrificed to allow for post-mortem neuropathological analyses exploring whether ATF4-controlled beclin-1 expression modulates htt aggregation and reduces neuronal loss. Brains were sectioned and compared to mice injected with ATF4-GFP. The brains for the remaining control groups (HD no vector, GFP, BECN1) have been sectioned, but further processing and analysis will be completed in the future.

DAB Staining

Brain sections were collected in series. Two adjacent series were used for immunostaining of GFP as a proxy to sensor-controlled expression and for ubiquitin, a marker of aggregation. Striatal sections were processed using a DAB staining protocol to visualize the presence of select proteins

via antibody processing. Tissue sections were placed in a PBS solution containing 3% hydrogen peroxide and 0.1% Triton X-100 to allow for permeabilization for 20 minutes, rinsed three times in PBS, then blocked with 4% normal donkey serum and 0.1% Triton X-100 in PBS for 30 minutes at room temperature. Following blocking and PBS rinses, tissue was transferred to a new dish and incubated with primary antibody solutions overnight at 4° C using a rabbit anti-GFP antibody (A11122 Thermo Fischer Scientific) and 2% normal donkey serum (017-000-121 Jackson ImmunoResearch) in PBS for one set of images and a rabbit anti-ubiquitin antibody (Z0458 DAKO) with 2% normal donkey serum in PBS for the second set of images. After three washes in PBS, the tissue was transferred to a solution containing 2% normal donkey serum and biotinylated anti-rabbit antibody (711-065-152 Jackson Immune Research) at a concentration of 1:1000 for one hour. After several rinses in PBS, sections were transferred to the tertiary solution containing an avidin-biotin complex (PK-4000 Vector Laboratories) for overnight incubation at 4° C. Following rinsing, tissue was stained in a PBS-based solution containing 0.012g of diaminobenzidine tetrahydrochloride (DAB; Sigma, St Louis, MO, USA) and 1 µL of hydrogen peroxide for 12 minutes until a dark brown reaction product was visible.

Imaging

Slides from R6/2 mice that were stained with GFP and BECN1 vectors were imaged. Images were obtained using the Cytation 5 Imaging Reader system from BioTek to capture montages of striatal sections for each mouse with bright field contrast at 10X magnification. Montages were stitched together and saved for further analysis.

Image Analysis

Images were analyzed using Fiji software (ImageJ.net, NIH). Slides stained with GFP were assessed to select the brain slice from each slide with the most distinct staining. Upon selection, the section from the GFP stained slides was matched to its adjacent section stained using ubiquitin. Images were then opened in Fiji to identify the region within which the viral vectors spread using the GFP slides. The corresponding region was used to create a mask to overlay the corresponding region within the ubiquitin-stained section. Once the area of the ubiquitin-stained section was identified for each mouse in the ATF4-GFP and ATF4-BECN1 treatment groups, a region of interest (ROI) was created to count the number of ubiquitinated htt aggregates per ROI. Ten ROI within each section were selected randomly to perform counts.

Statistical Analysis

Behavioral data were analyzed using Prism statistical software. The objective of statistical analyses was to determine the potential relationship between treatment groups and disease progression over time. A two-way repeated measures analysis of variance (ANOVA) was used to compare the differences in behavior amongst R6/2 mice injected with ATF4-GFP, ATF4-BECN1, GFP, BECN1, or no vector, as well as wild type control mice. All tests were conducted using a significance level of 0.05 to evaluate possible group differences in rearing behavior, climbing, and the average amount of time spent on the mesh per climb. Analyses for behavioral tests were isolated to weeks 5 through 10 due to being unable to obtain data for later weeks from all mice because of disease progression and death of mice. Aggregate counts between ATF4-GFP and ATF4-BECN1 treated mice were performed using Prism statistical software to determine if there

was a significant difference in htt aggregates between treatment groups (ATF4-GFP or ATF4-BECN1). An unpaired t-test comparing the average number of aggregates present per ROI within the ATF4-GFP group or ATF4-BECN1 group respectively was conducted with a significance level of 0.05. Results are presented as mean +/- SEM unless otherwise stated.

Results

To assess the validity of our hypothesis, we considered a combination of assessments to measure disease progression, motor skills, and post-mortem neuropathology. All values are reported as the mean $\pm$ the standard error of the mean. R6/2 mice across treatment groups were weighed twice a week beginning one-week post injections, with values averaged to track changes in weight over time. For analysis, the average weight from all the mice within each treatment group was compared over time (Figure 2). Weight was measured as an indicator of disease progression. Our data shows that R6/2 mice started to lose weight around week 9. This is consistent with data from other studies showing that R6/2 mice experience significant muscle atrophy starting around 8 weeks of age[66]. We did not see any difference in weight decline amongst the treatment groups (ATF4-GFP, ATF4-BECN1, GFP, BECN1, HD no virus).

To assess climbing and rearing behavior, mice were placed in a wire mesh enclosure for a 10-minute period. To test motor skills, we analyzed climbing behavior, rearing, and movement on the mesh. Data was collected for wild-type mice and R6/2 mice beginning one-week post viral intrastriatal injections. Results were averaged across all mice within each treatment or control group for each week. From weeks 5 to 13, wild-type mice gradually improved in climbing abilities

and had an increase in their average number of climbs from 24.6 ± 1.5 to 38.0 ± 2.4. Although variable, the untreated R6/2 mice showed a reduced number of climbs compared to wild-type mice beginning at week 5 with an average of 16.3 ± 8.0 climbs at week 5 which continued to decline over the 9-week period to approximately 1.0 ± 0.7 climbs per trial. The treated R6/2 groups similarly showed a reduced number of climbs compared to the wild-type mice, with a range between 5 and 10 climbs at week 5 followed by a steady decline. We did not see a significant difference amongst the viral vector treatment groups (ATF4-GFP, ATF4-BECN1, GFP, BECN1) at any age with regard to the average number of climbs during the 10-minute period (Figure 3). However, wild-type mice had significantly more climbs than treated R6/2 mice at all time points included in statistical analyses (weeks 5-10, $p<0.05$). Wild-type mice performed significantly better than untreated R6/2 mice at weeks 6, 8, 9, and 10.

Similarly, amongst viral vector treatment groups, we did not observe a significant difference in rearing events and R6/2 mice had a distinct decline in the average number of rearing events over time (Figure 4). Rearing events for wild-type mice were more variable over the 9 weeks, but the average number of rearing events did not change significantly between weeks 5 and 13 with the mice initially having 26.4 ± 0.9 rearing events and later 26.6 ± 1.0 rearing events. In contrast, both treated and untreated R6/2 mice experienced a gradual decline between weeks 5 and 13. Treated R6/2 mice showed a similar number of rearing events at week 5 when compared to wild-type, with average number ranging from 24.5 ± 1.1 to 28.0 ± 1.4 approximately prior to declining to between 4.0 ± 1.0 and 7.0 ± 1.0 by week 13. Initially, untreated mice had slightly fewer rearing events with approximately 21.0 ± 2.6 on average at week 5 and declined to about 7.0 ± 2.7 rearing

events at week 13. For weeks 8 through 10, there were statistically significant differences between the R6/2 treatment groups and the wild type mice for rearing behavior, with wild-type mice having significantly more rearing events than R6/2 groups ($p<0.05$).

To measure movement once on the mesh, we examined the average amount of time spent on the mesh per each full climb for both wild-type and R6/2 mice over time. Wild-type mice experienced less variability than R6/2 mice in terms of the amount of time spent moving on the mesh per climb, averaging between 3.30 ± 0.16 and 4.15 ± 0.34 seconds per climb over the 9-week period. For several time points, wild-type mice spent less time on the mesh on average than R6/2 mice, which is likely attributable to the R6/2 mice appearing stuck on the wire for prolonged periods of time. In contrast to the consistency of wild-type mice, both treated and untreated R6/2 mice had significantly more variability over the 9 weeks, but especially during the last 4 weeks of testing. For example, R6/2 mice spent between 3.35 ± 1.12 and 6.17 ± 0.90 seconds on the mesh per climbing at week 5, compared to an average between 1.67 ± 1.67 and 7.0 ± 6.5 seconds per climb at week 13. We did not observe any significant difference amongst any of the R6/2 or wild-type groups of mice (ATF4-GFP, ATF4-BECN1, GFP, BECN1, HD no virus, WT) regarding time spent on the mesh (Figure 5).

Following completion of the behavioral portion of assessments, brain sections were collected and processed to analyze the presence of ubiquitinated huntingtin aggregates. For comparison purposes, ATF4-GFP and ATF4-BECN1 groups were selected to assess the effect of the treatment, BECN1, coupled with ATF4-modulation to a control group that lacked the respective treatment.

Given difficulty in visualizing the fluorescent tag especially in the tissue from the ATF4-BECN1 treated mice, tissue was stained with DAB for amplification of the GFP signal to improve visualization. Tissue sections were stained using either GFP or ubiquitin specific antibodies to reveal treatment expression and htt aggregates, respectively. For both treatments, ATF4 controlled transgene expression (GFP or BECN1-GFP) was restricted along the injection tract with little spread to other parts of the striatum (Figure 6A-B). In sections from the ATF4-GFP treatment group, GFP was present in cell bodies, dendrites, and axons, and filled both the cytoplasm and nuclei of the expressing neurons (Figure 6A). Within the ATF4-BECN1 group, GFP was localized similarly except for very little expression seen in nuclei (Figure 6A, C). Expression was notable in all cell types for both ATF4-GFP and ATF4-BECN1 treatment groups, regardless of cell shape or size (Figure 6A-D). For both treatment groups, ubiquitin aggregates were visible throughout the entire tissue section, including cortex and striatum (Figure 6B, D). On average, ATF4-GFP mice had 9.52 ± 0.53 htt aggregates per ROI. ATF4-BECN1 mice had significantly fewer aggregates with only 5.45 ± 0.68 per ROI (t-test, $p = 0.0019$).

Discussion

We utilized an R6/2 mouse model to investigate the effects of ATF4-controlled release of the autophagy inducer BECN1 on behavior and neuropathology associated with Huntington's disease. To examine changes in behavior and measure disease progression, R6/2 and wild type mice performed climbing assessments, clasping assessments, and were weighed over several weeks. The ATF4-BECN1 treatment did not significantly improve climbing or rearing abilities in mice, which was not consistent with our hypothesis. Rather, the only statistically significant

variation in climbing and rearing behavior as measured via the climbing assay was between wild type mice and the R6/2 mice groups. These results, coupled with the lack of significant spreading of the viral vector outside the area of injection, suggest the therapy did not have as significant of a reach as intended in terms of therapeutic efficacy. While there was a significant difference between ATF4-GFP mice and ATF4-BECN1 mice with regard to the number of aggregates present in areas the treatment reached, the lack of spreading to further regions of the tissue could explain the lack of variation in motor skills. The small spread of viral vectors is consistent with prior data on AAV2 suggesting it spreads less when compared with AAV 1, 5, 8, and 9[67]. Given that AAV2 was the adeno-associated viral vector serotype utilized throughout this study, future considerations include use of AAV5 or another serotype with greater spread to ensure the vector is farther reaching within the neuronal tissue.

Another consideration is the difficulty of translating results from in vitro models to the in vivo R6/2 model. In comparison to the disease progression in humans over the course of approximately 15 years, the R6/2 model exhibits a very fast period of progression, with mice living an average of 13-16 weeks and severe impairments beginning between 8 and 12 weeks[68]. The analysis of mouse weights, which showed an initial increasing trend until approximately 4-5 weeks after injections followed by a decline, is consistent with worsening conditions due to HD progression. The severity of symptoms and fast disease progression represents a potential downside to the usage of the R6/2 model, especially as compared to the R6/1 transgenic mouse model. The R6/1 model was developed in the same way as R6/2 mice, but involves the insertion of a gene with only 116 CAG repeats, producing a milder behavioral phenotype[65]. Given that R6/2

mice did not receive injections of viral vectors until week 4, it is possible that there was not enough time to develop a robust response from the treatment vectors.

For the same reason, it might be beneficial to explore this therapy in models with a slower disease progression that is more consistent with the disease in humans and offers sufficient time for the gene therapy to work. One such example is the yeast artificial chromosome (YAC) transgenic mouse model, which recapitulates the expanded polyglutamine tract in accordance with human neuropathology. The YAC128 model contains 128 CAG repeats and mimics human disease progression via selective, age-dependent brain atrophy and the development of motor abnormalities[69]. Analysis of the YAC128 model suggests a slower disease progression, with initial hyperkinesia manifesting at 3 months followed by motor skill deficits originating at 6 months prior to progression to hypokinesia by 12 months[69]. Neuropathologically, mice exhibit initial striatal atrophy by 9 months, cortical atrophy at approximately 12 months, and continued loss of striatal neurons and striatal cell surface area as time progresses[69]. Given the prolonged period of disease progression and consistency with regard to neurological and behavioral deficits, the YAC128 model affords an opportunity to examine the efficacy of the treatment over a timeline that better aligns with human disease.

Along with concerns regarding the timeline of the R6/2 model used in our study, the treatment did not appear to spread significantly beyond the striatal area within which it was directly injected. An additional option would be the injection of viral vectors into cerebral ventricles as opposed to the striatum to allow the treatment to extend more globally within the brain.

Previous studies have elucidated the ability of AAV to move from cerebral ventricles into brain parenchyma during the first 12-24 hours after birth in neonatal mice, prior to complete development of the ependymal lining[70]. Injection of AAV into newborn mice was shown to produce widespread neuronal transduction and expression within the first several days that persists over the entire lifetime of the mouse[70]. As a result, earlier injections into the ventricles may enhance the ability of ATF4-BECN1 to reduce htt aggregate loads throughout neuronal tissue and reduce symptomatic progression.

Neuropathological assessments were performed in ATF4-BECN1 and ATF4-GFP groups to examine differences between the primary therapy group and a control group. Following DAB staining, image processing, and image analysis, results illustrated significantly fewer aggregates in the ATF4-BECN1 group compared to the ATF4-GFP treatment group, which coincides with our hypothesis. Coupled with confirmation that GFP and BECN1 were both expressed when coupled with the ATF4 sensor, this data suggests the AAV may be working at a cellular level. Based on our hypothesis that BECN1 is reducing stress by clearing htt aggregates and its expression is modulated by ATF4 sensing stress, the level of therapy should decrease as well. This may explain the lower levels of BECN1 expression in the ATF4-BECN1 group, but should be tested further by assessing BECN1 levels via a BECN1 antibody[71]. Quantification of the presence of BECN1 in ATF4-BECN1 treated mice compared to BECN1 or ATF4-GFP mice would offer insight into the importance of the ATF4 sensor with regard to therapeutic modulation.

Further, the neuropathological data is consistent with results obtained from in vitro assessments examining AAV-based expression vectors in HEK293 cells[72]. Preliminary studies illustrated a robust response of a reduction in htt-Q150 load in cells expressing both htt and ATF4-BECN1[72]. In comparison to HEK293 cells expressing BECN1 in the absence of ATF4, similar levels of activity were observed with regard to a reduction in htt-Q150[72]. Given that the therapy appeared to work at a cellular level as indicated by the decreased presence of htt aggregates, the treatment is promising despite being insufficient to produce significant changes in behavioral symptoms. As such, future directions include continued neuropathological staining and analysis for the remaining treatment groups (GFP, BECN1, HD no virus) and control groups (wild type) to draw comparisons with regard to htt aggregation and viral vector distribution within the brain.

Figures

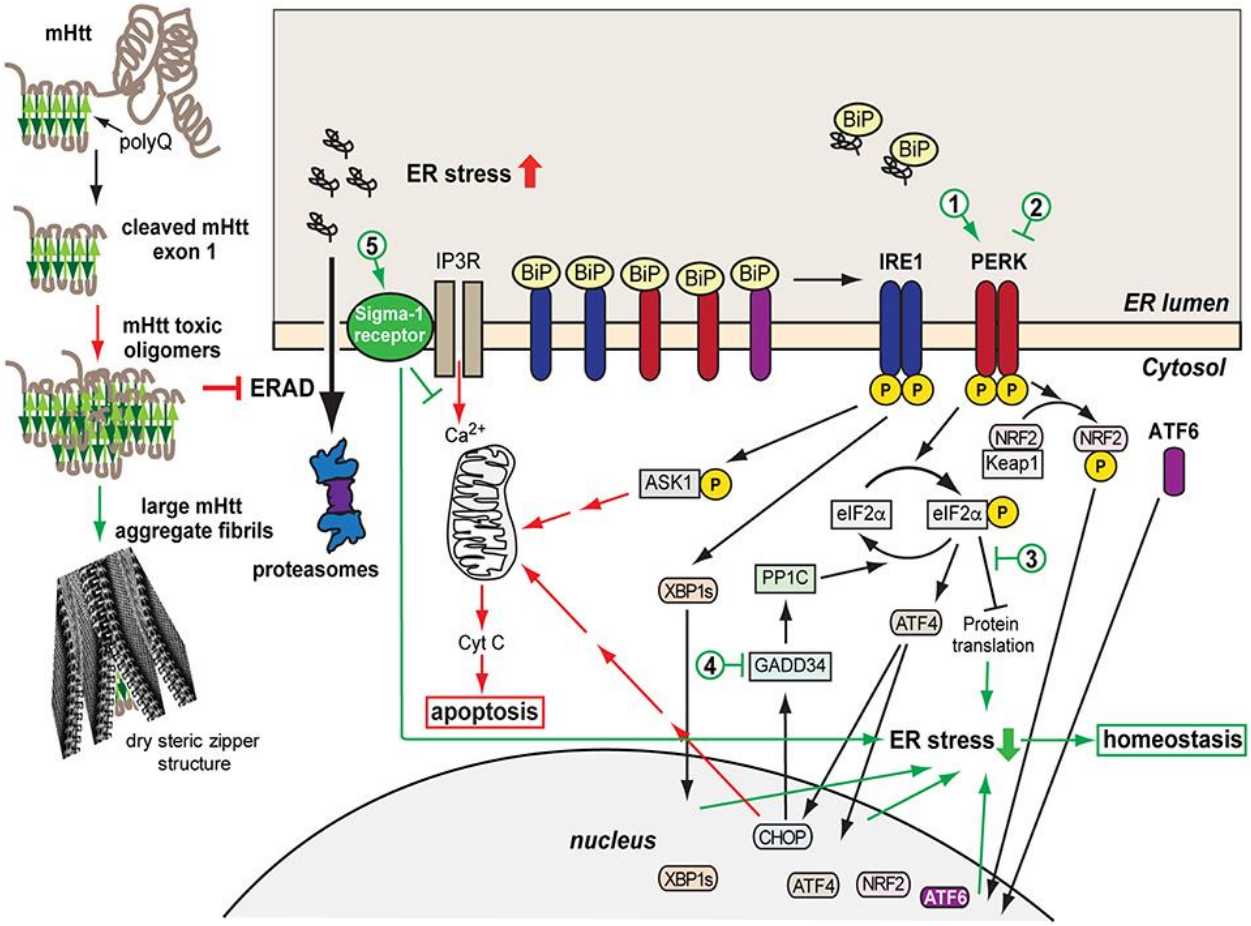

Figure 1: **Modeling the relationship between mHTT aggregation, ER stress, and the UPR.**[28]

The mutant protein contributes to ER stress due to the elongated polyQ tract, which is cleaved at exon 1 to form toxic oligomers. These oligomers aggregate, cause sequestration of ERAD factors, and result in a reduction in ERAD proteins, such as p97. ERAD inhibition leads to an accumulation of other unfolded secretory proteins and subsequent ER stress, thereby activating the UPR through IRE1, PERK, and ATF6 pathways. Red arrows indicate cytotoxic pathways, while protective pathways are shown in green. Reprinted from "Protein Misfolding and ER Stress in Huntington's Disease," by T. Shacham and N. Sharma, 2019, Frontiers in Molecular Biosciences, 6. Copyright 2019 by Shacham, Sharma and Lederkremer.

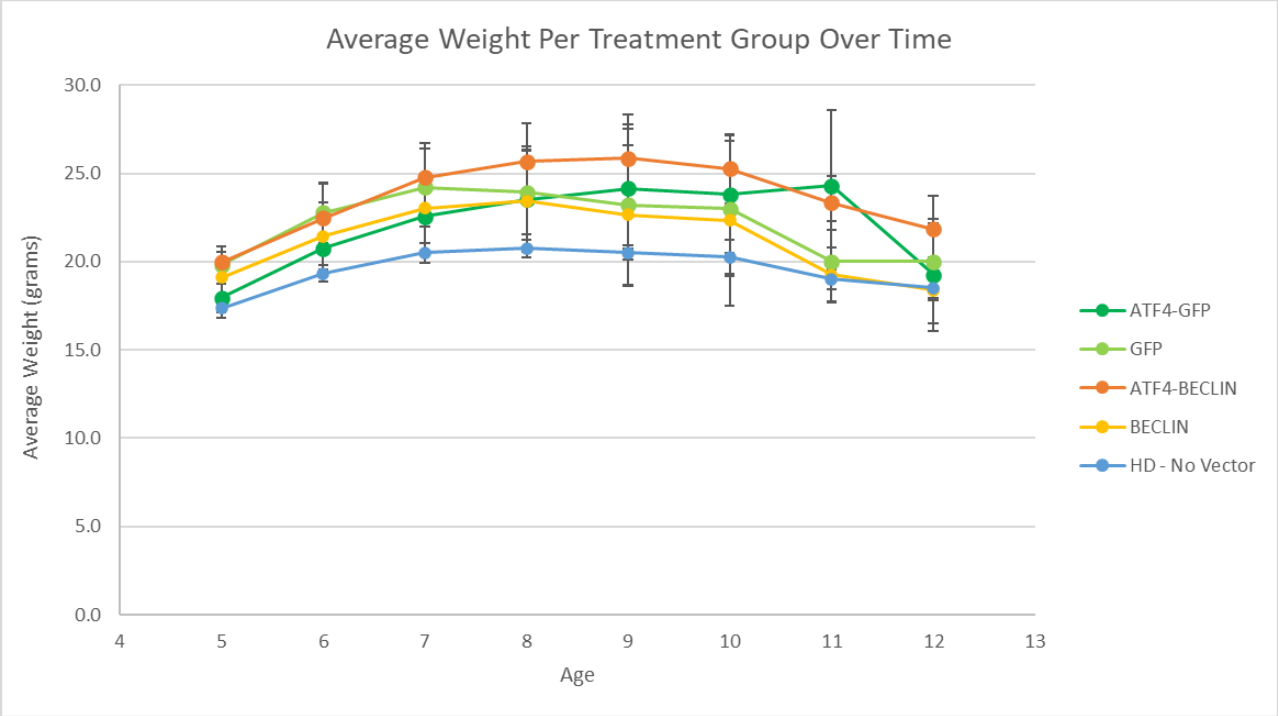

Figure 2: **Effect of Treatment on Average Weights.** This graph illustrates the average weight of mice per treatment group over time. There was no significant difference amongst the treatment and control groups shown (ATF4-GFP, ATF4-BECN1, GFP, BECN1, HD no virus).

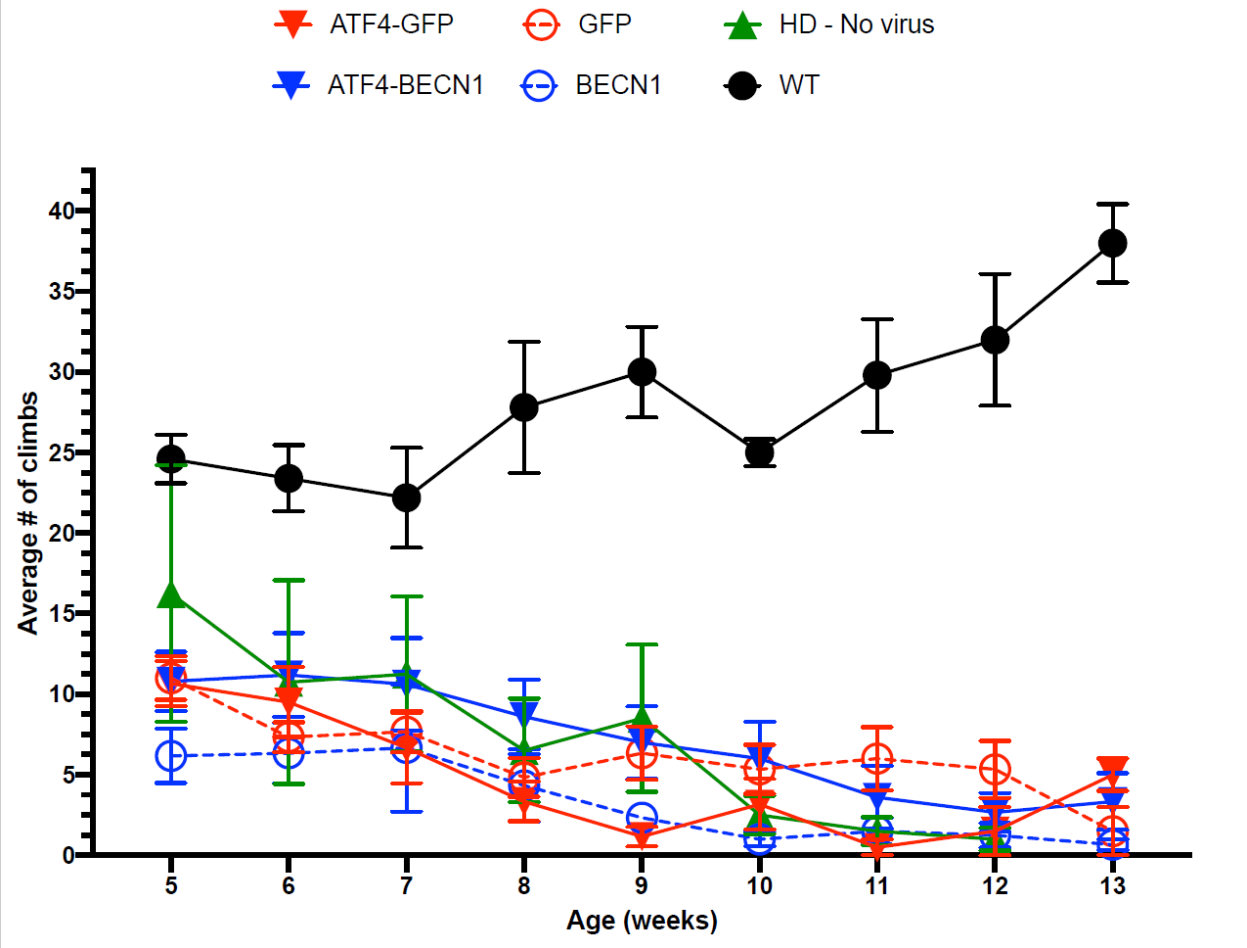

Figure 3: **Effect of Treatment on Climbing Events.** This graph illustrates the average number of climbs per treatment group over time. There was no significant difference amongst the viral vector treatment groups (ATF4-GFP, ATF4-BECN1, GFP, BECN1).

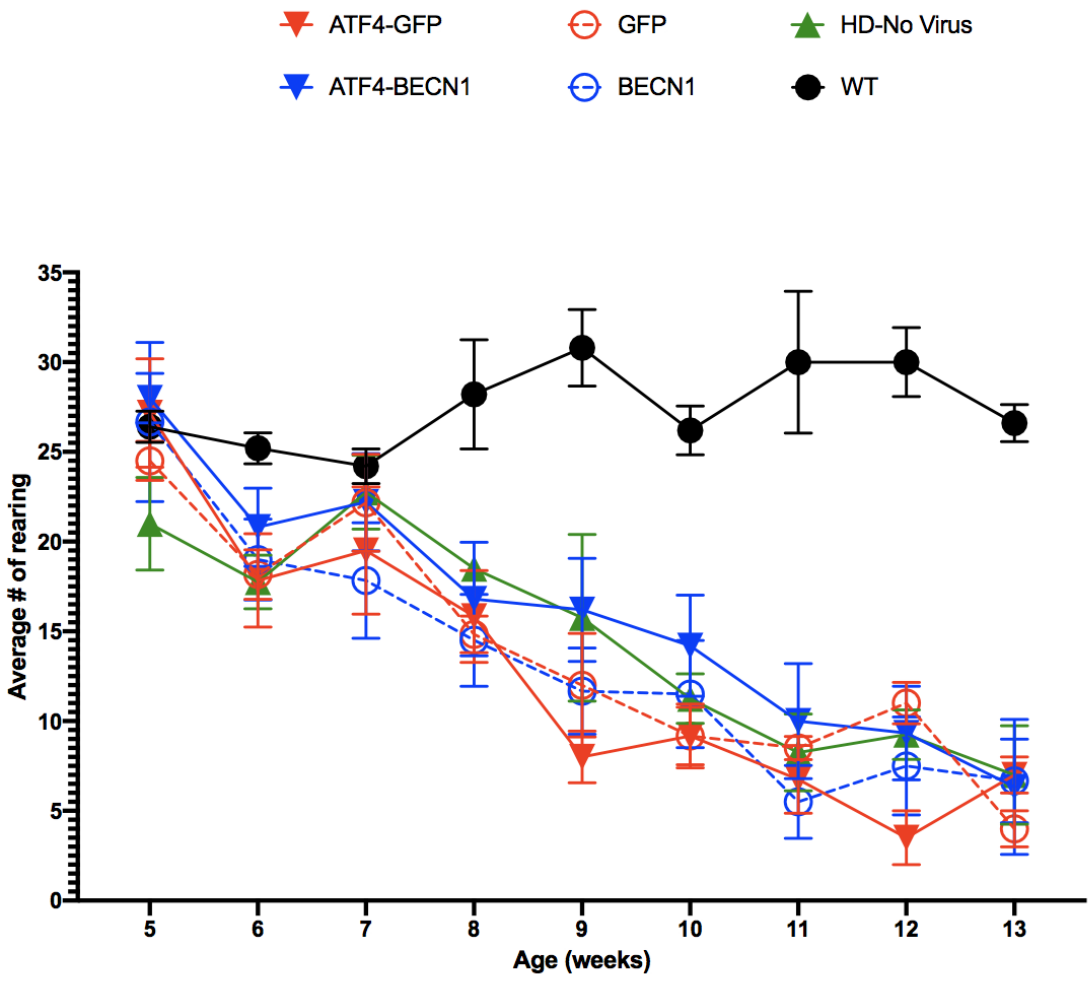

Figure 4: **Effect of Treatment on Rearing Events.** This graph illustrates the average number of rearing attempts per treatment group over time. There was no significant difference amongst the viral vector treatment groups (ATF4-GFP, ATF4-BECN1, GFP, BECN1).

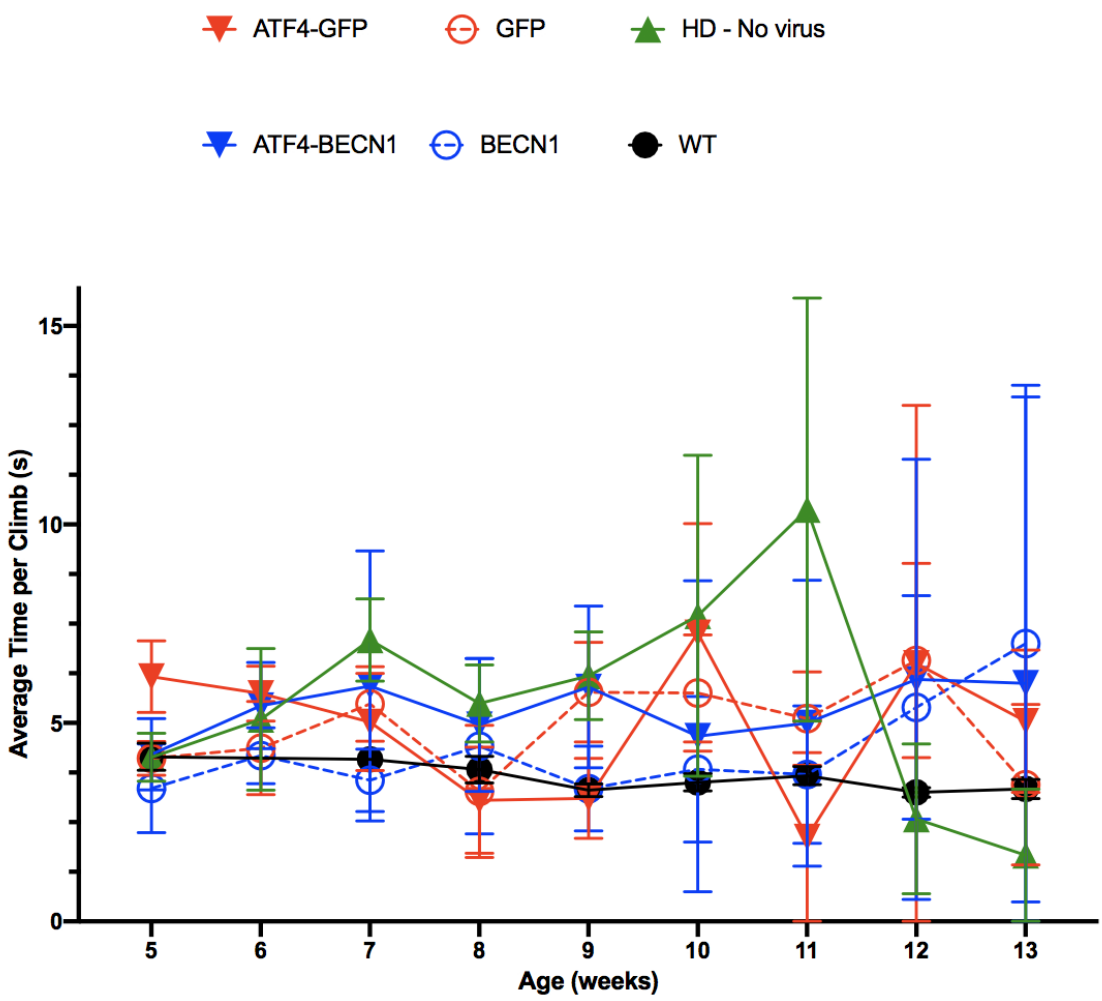

Figure 5: **Effect of Treatment on Time Spent on Mesh.** This graph shows the average amount of time spent on the mesh per climb for each treatment group over time. There was no significant difference amongst any of the treatment or control groups shown (ATF4-GFP, ATF4-BECN1, GFP, BECN1, WT, HD no virus).

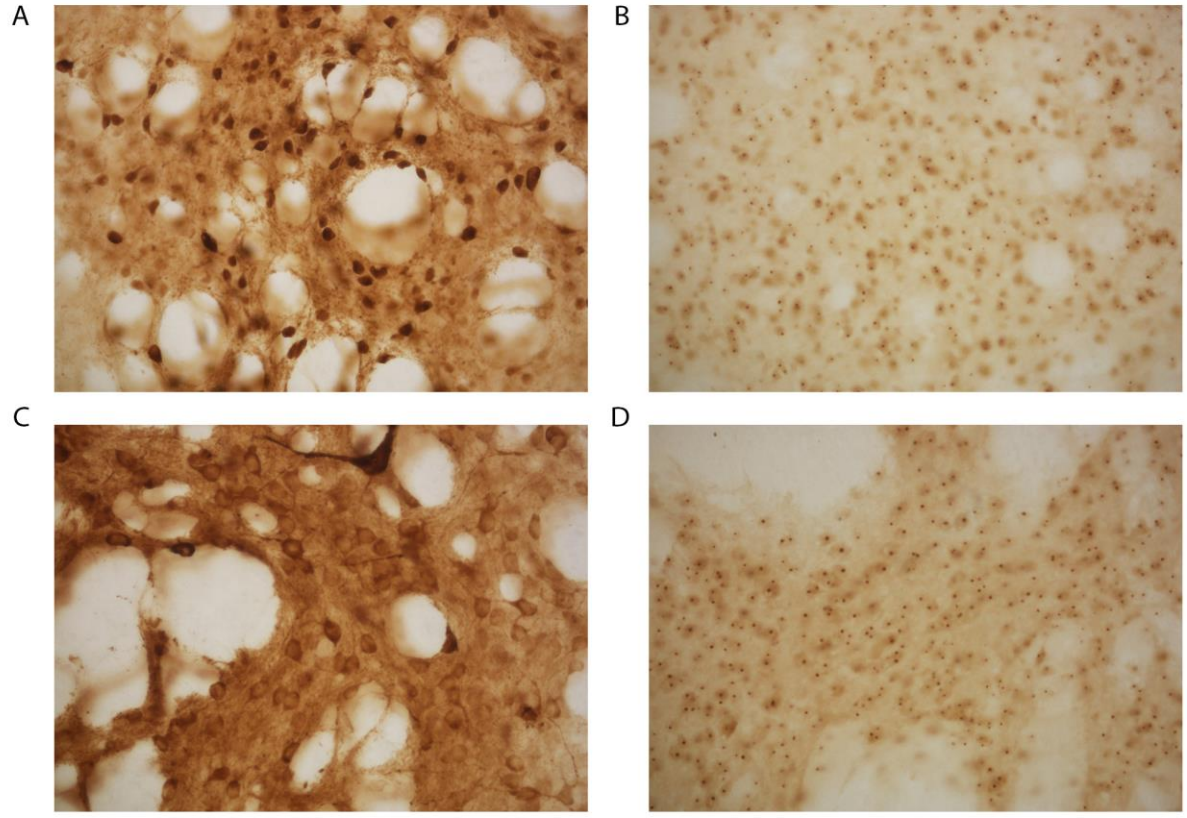

Figure 6: **GFP and Ubiquitin expression in the striatum of R6/2 mice expressing ATF4-GFP and ATF4-BECN1.** Micrographs showing GFP (A, C) and Ubiquitin (B, D) immunostaining in the striatum of R6/2 mice from the ATF4-GFP treatment group (A-B) and ATF4-BECN1 treatment group (C-D).

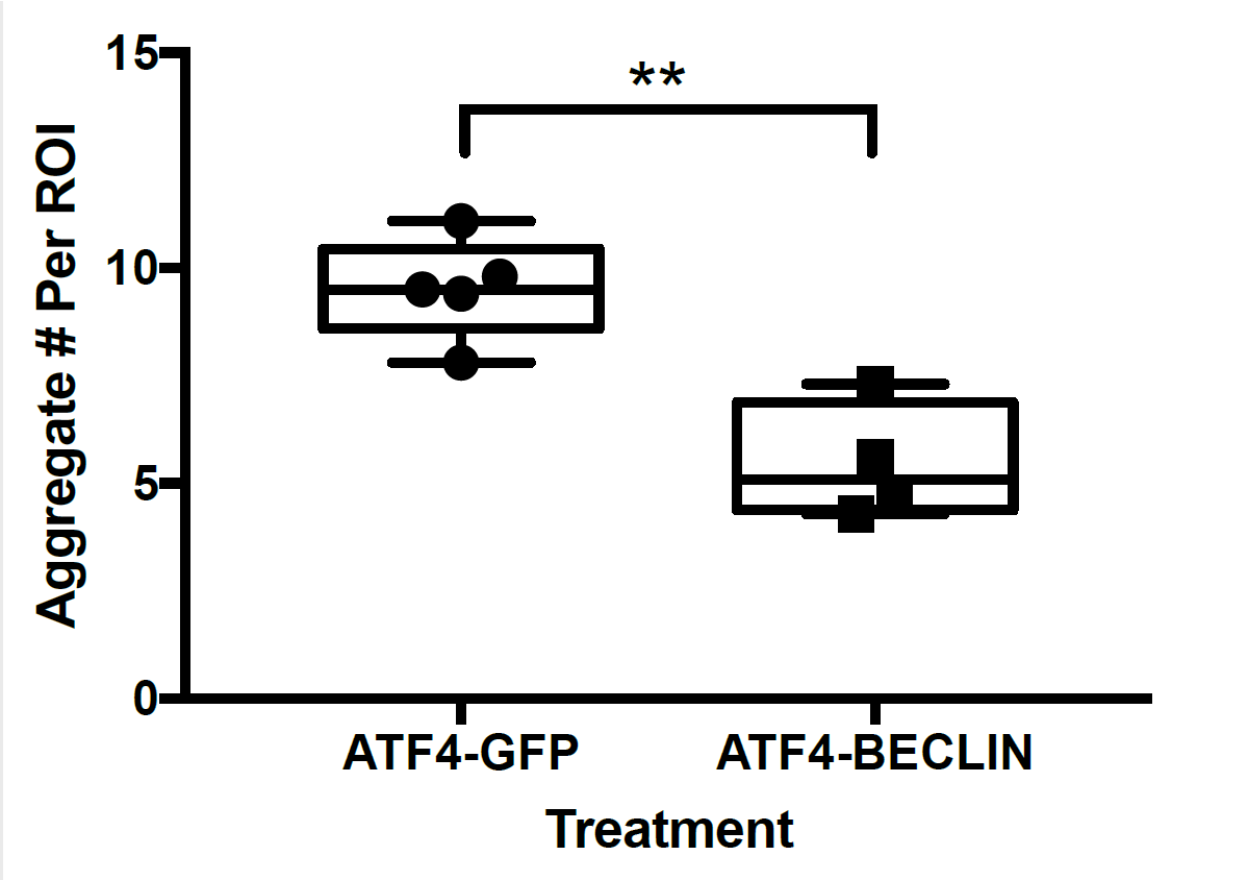

Figure 7: **ATF4-BECLIN Reduces Aggregate Load in R6/2 Mice.** This graph illustrates the average number of ubiquitinated htt aggregates present in ATF4-GFP and ATF4-BECLIN treatment groups. Data points represent the average for each mouse within their treatment group as calculated from 10 individual ROI measures per mouse. A total of 5 mice were included for the ATF4-GFP group and 4 mice were included for analysis for the ATF4-BECLIN group. **: t-test $p < 0.01$

Supplementary Data

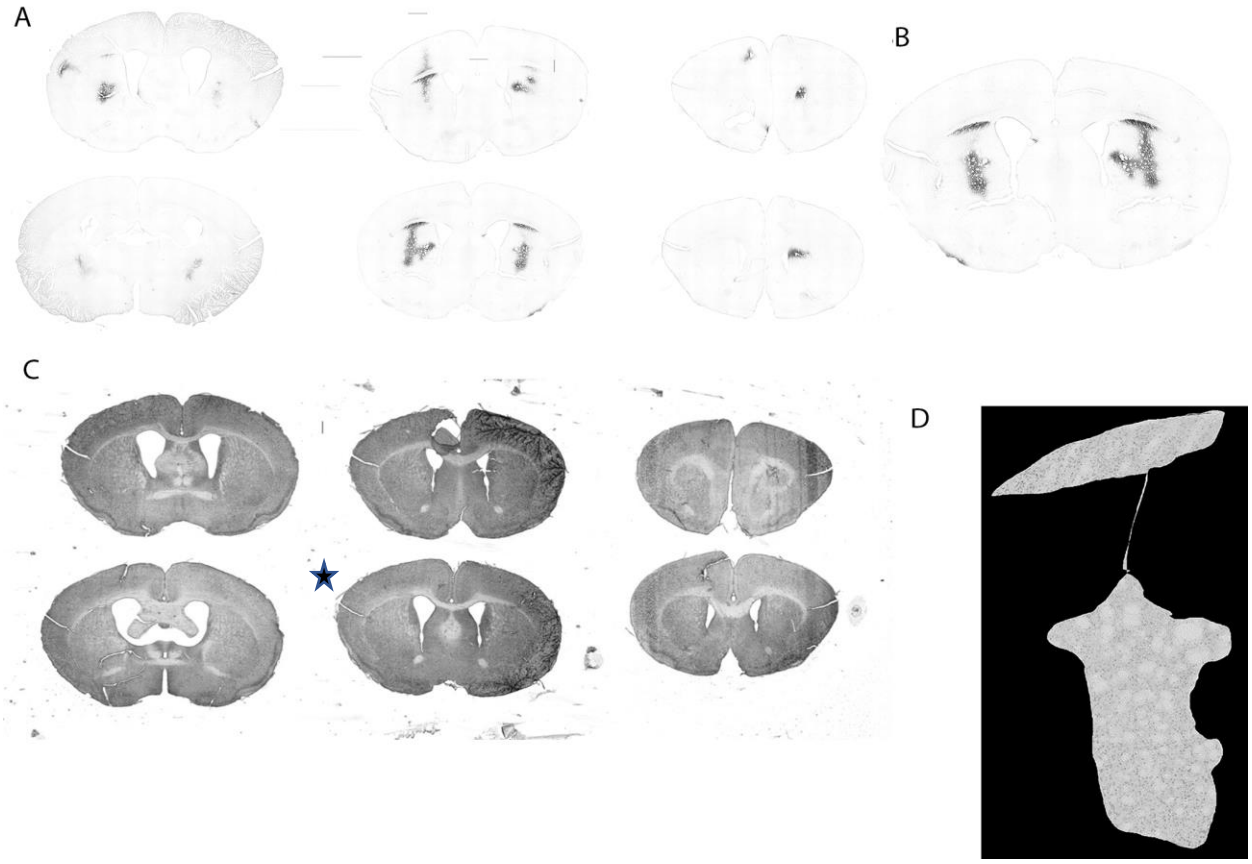

Figure S1: **Aggregate Count Methodology.** This figure illustrates the steps taken for aggregate counts within the treatment area for an R6/2 mouse in the ATF4-GFP group. (A) Sections from one well stained with anti-GFP (B) Brain section selected for further analysis due to clarity of vector spread (C) Sections from an adjacent well stained with anti-ubiquitin. Section corresponding to section in B is indicated by the star. (D) Mask created from the GFP-stained section overlayed on corresponding ubiquitin section to highlight the area within which the viral vector was present.

References

1. Bashir, H. Emerging therapies in Huntington's disease. Expert Review of Neurotherapeutics (2019) doi:10.1080/14737175.2019.1631161.
2. Caron, N. S., Dorsey, E. R. & Hayden, M. R. Therapeutic approaches to huntington disease: From the bench to the clinic. Nature Reviews Drug Discovery (2018) doi:10.1038/nrd.2018.133.
3. Huntington, T. et al. A novel gene containing a trinucleotide repeat that is expanded and unstable on Huntington's disease chromosomes. The Huntington's Disease Collaborative Research Group. Cell (1993) doi:10.1016/0092-8674(93)90585-E.
4. Saudou, F. & Humbert, S. The Biology of Huntingtin. Neuron (2016) doi:10.1016/j.neuron.2016.02.003.
5. Halliday, G. M. et al. Regional specificity of brain atrophy in Huntington's disease. Exp. Neurol. (1998) doi:10.1006/exnr.1998.6919.
6. Albin, R. L. Selective neurodegeneration in Huntington's disease. Annals of Neurology (1995) doi:10.1002/ana.410380602.
7. Aylward, E. H. et al. Longitudinal change in basal ganglia volume in patients with Huntington's disease. Neurology (1997) doi:10.1212/WNL.48.2.394.
8. Hedreen, J. C. & Folstein, S. E. Early loss of neostriatal striosome neurons in huntingtons disease. J. Neuropathol. Exp. Neurol. (1995) doi:10.1097/00005072-199501000-00013.
9. Reiner, A. et al. Differential loss of striatal projection neurons in Huntington disease. Proc. Natl. Acad. Sci. U. S. A. (1988) doi:10.1073/pnas.85.15.5733.
10. Gutekunst, C. A. & Norflus, F. Huntington's disease. in Protein Misfolding in Neurodegenerative Diseases: Mechanisms and Therapeutic Strategies (2007). doi:10.17816/2686-8997-2020-1-3-139-158.
11. Hilditch-Maguire, P. et al. Huntingtin: An iron-regulated protein essential for normal nuclear and perinuclear organelles. Hum. Mol. Genet. (2000) doi:10.1093/hmg/9.19.2789.
12. Velier, J. et al. Wild-type and mutant huntingtins function in vesicle trafficking in the secretory and endocytic pathways. Exp. Neurol. (1998) doi:10.1006/exnr.1998.6832.
13. Li, J. Y., Plomann, M. & Brundin, P. Huntington's disease: A synaptopathy? Trends Mol. Med. (2003) doi:10.1016/j.molmed.2003.08.006.
14. Jones, L. & Hughes, A. Pathogenic mechanisms in huntington's disease. in International Review of Neurobiology (2011). doi:10.1016/B978-0-12-381328-2.00015-8.
15. Bates, G. P. et al. Huntington disease. Nature Reviews Disease Primers (2015) doi:10.1038/nrdp.2015.5.
16. Ross, C. A. & Tabrizi, S. J. Huntington's disease: From molecular pathogenesis to clinical treatment. The Lancet Neurology (2011) doi:10.1016/S1474-4422(10)70245-3.
17. Travessa, A. M., Rodrigues, F. B., Mestre, T. A. & Ferreira, J. J. Fifteen years of clinical trials in Huntington's disease: A very low clinical drug development success rate. J. Huntingtons. Dis. (2017) doi:10.3233/JHD-170245.
18. Soares, T. R., Reis, S. D., Pinho, B. R., Duchen, M. R. & Oliveira, J. M. A. Targeting the proteostasis network in Huntington's disease. Ageing Research Reviews (2019) doi:10.1016/j.arr.2018.11.006.

19. Hipp, M. S., Park, S. H. & Hartl, U. U. Proteostasis impairment in protein-misfolding and -aggregation diseases. Trends in Cell Biology (2014) doi:10.1016/j.tcb.2014.05.003.
20. Sieradzan, K. A. et al. Huntington's disease intranuclear inclusions contain truncated, ubiquitinated huntingtin protein. Exp. Neurol. (1999) doi:10.1006/exnr.1998.7005.
21. Waelter, S. et al. Accumulation of mutant huntingtin fragments in aggresome-like inclusion bodies as a result of insufficient protein degradation. Mol. Biol. Cell (2001) doi:10.1091/mbc.12.5.1393.
22. Matthias E, F., Ravi Kiran Reddy, K., Joaquin, G. L., Susana, M. & Kameshwar RS, A. The unfolded protein response and its potential role in Huntington's disease elucidated by a systems biology approach. F1000Research (2015) doi:10.12688/f1000research.6358.2.
23. Reijonen, S., Putkonen, N., Nørremølle, A., Lindholm, D. & Korhonen, L. Inhibition of endoplasmic reticulum stress counteracts neuronal cell death and protein aggregation caused by N-terminal mutant huntingtin proteins. Exp. Cell Res. (2008) doi:10.1016/j.yexcr.2007.12.025.
24. Tang, T. S. et al. Huntingtin and huntingtin-associated protein 1 influence neuronal calcium signaling mediated by inositol-(1,4,5) triphosphate receptor type 1. Neuron (2003) doi:10.1016/S0896-6273(03)00366-0.
25. Donnelly, N., Gorman, A. M., Gupta, S. & Samali, A. The eIF2α kinases: Their structures and functions. Cellular and Molecular Life Sciences (2013) doi:10.1007/s00018-012-1252-6.
26. Dey, S. et al. Both transcriptional regulation and translational control of ATF4 are central to the integrated stress response. J. Biol. Chem. (2010) doi:10.1074/jbc.M110.167213.
27. Moon, S. L., Sonenberg, N. & Parker, R. Neuronal Regulation of eIF2α Function in Health and Neurological Disorders. Trends in Molecular Medicine (2018) doi:10.1016/j.molmed.2018.04.001.
28. Shacham, T., Sharma, N. & Lederkremer, G. Z. Protein misfolding and ER stress in Huntington's disease. Frontiers in Molecular Biosciences (2019) doi:10.3389/fmolb.2019.00020.
29. Schröder, M. & Kaufman, R. J. The mammalian unfolded protein response. Annual Review of Biochemistry (2005) doi:10.1146/annurev.biochem.73.011303.074134.
30. Harding, H. P., Zhang, Y. & Ron, D. Protein translation and folding are coupled by an endoplasmic-reticulum-resident kinase. [see comments.] [erratum appears in Nature 1999 Mar 4;398(6722):90.]. Nature (1999).
31. Blais, J. D. et al. Activating Transcription Factor 4 Is Translationally Regulated by Hypoxic Stress. Mol. Cell. Biol. (2004) doi:10.1128/mcb.24.17.7469-7482.2004.
32. Amodio, G. et al. Endoplasmic reticulum stress reduces the export from the ER and alters the architecture of post-ER compartments. Int. J. Biochem. Cell Biol. (2009) doi:10.1016/j.biocel.2009.08.006.
33. Zinszner, H. et al. CHOP is implicated in programmed cell death in response to impaired function of the endoplasmic reticulum. Genes Dev. (1998) doi:10.1101/gad.12.7.982.
34. Ohoka, N., Yoshii, S., Hattori, T., Onozaki, K. & Hayashi, H. TRB3, a novel ER stress-inducible gene, is induced via ATF4-CHOP pathway and is involved in cell death. EMBO J. (2005) doi:10.1038/sj.emboj.7600596.
35. Duennwald, M. L. & Lindquist, S. Impaired ERAD and ER stress are early and specific

events in polyglutamine toxicity. Genes Dev. (2008) doi:10.1101/gad.1673408.
36. Ye, Y., Meyer, H. H. & Rapoport, T. A. Function of the p97-Ufd1-Npl4 complex in retrotranslocation from the ER to the cytosol: Dual recognition of nonubiquitinated polypeptide segments and polyubiquitin chains. J. Cell Biol. (2003) doi:10.1083/jcb.200302169.
37. Nath, S., Munsie, L. N. & Truant, R. A huntingtin-mediated fast stress response halting endosomal trafficking is defective in Huntington's disease. Hum. Mol. Genet. (2015) doi:10.1093/hmg/ddu460.
38. Li, W. & Ye, Y. Polyubiquitin chains: Functions, structures, and mechanisms. Cellular and Molecular Life Sciences (2008) doi:10.1007/s00018-008-8090-6.
39. Li, X. J. & Li, S. Proteasomal dysfunction in aging and Huntington disease. Neurobiology of Disease (2011) doi:10.1016/j.nbd.2010.11.018.
40. Wang, J. et al. Impaired ubiquitin-proteasome system activity in the synapses of Huntington's disease mice. J. Cell Biol. (2008) doi:10.1083/jcb.200709080.
41. Díaz-Hernández, M. et al. Inhibition of 26S proteasome activity by huntingtin filaments but not inclusion bodies isolated from mouse and human brain. J. Neurochem. (2006) doi:10.1111/j.1471-4159.2006.03968.x.
42. Harding, R. J. & Tong, Y. F. Proteostasis in Huntington's disease: Disease mechanisms and therapeutic opportunities. Acta Pharmacologica Sinica (2018) doi:10.1038/aps.2018.11.
43. Martinez-Vicente, M. et al. Cargo recognition failure is responsible for inefficient autophagy in Huntington's disease. Nat. Neurosci. (2010) doi:10.1038/nn.2528.
44. Wong, Y. C. & Holzbaur, E. L. F. The regulation of autophagosome dynamics by huntingtin and HAP1 is disrupted by expression of mutant huntingtin, leading to defective cargo degradation. J. Neurosci. (2014) doi:10.1523/JNEUROSCI.1870-13.2014.
45. Williams, A. et al. Novel targets for Huntington's disease in an mTOR-independent autophagy pathway. Nat. Chem. Biol. (2008) doi:10.1038/nchembio.79.
46. Rose, C. et al. Rilmenidine attenuates toxicity of polyglutamine expansions in a mouse model of Huntington's disease. Hum. Mol. Genet. (2010) doi:10.1093/hmg/ddq093.
47. Sarkar, S., Ravikumar, B., Floto, R. A. & Rubinsztein, D. C. Rapamycin and mTOR-independent autophagy inducers ameliorate toxicity of polyglutamine-expanded huntingtin and related proteinopathies. Cell Death and Differentiation (2009) doi:10.1038/cdd.2008.110.
48. Rui, Y. N. et al. Huntingtin functions as a scaffold for selective macroautophagy. Nat. Cell Biol. (2015) doi:10.1038/ncb3101.
49. Ashkenazi, A. et al. Polyglutamine tracts regulate beclin 1-dependent autophagy. Nature (2017) doi:10.1038/nature22078.
50. Yamanaka, T. et al. Mutant Huntingtin reduces HSP70 expression through the sequestration of NF-Y transcription factor. EMBO J. (2008) doi:10.1038/emboj.2008.23.
51. Neueder, A. et al. HSF1-dependent and-independent regulation of the mammalian in vivo heat shock response and its impairment in Huntington's disease mouse models. Sci. Rep. (2017) doi:10.1038/s41598-017-12897-0.
52. Hipp, M. S. et al. Indirect inhibition of 26S proteasome activity in a cellular model of Huntington's disease. J. Cell Biol. (2012) doi:10.1083/jcb.201110093.
53. Park, S. H. et al. PolyQ proteins interfere with nuclear degradation of cytosolic proteins

by sequestering the Sis1p chaperone. Cell (2013) doi:10.1016/j.cell.2013.06.003.
54. Yu, A. et al. Protein aggregation can inhibit clathrin-mediated endocytosis by chaperone competition. Proc. Natl. Acad. Sci. U. S. A. (2014) doi:10.1073/pnas.1321811111.
55. Neef, D. W., Turski, M. L. & Thiele, D. J. Modulation of heat shock transcription factor 1 as a therapeutic target for small molecule intervention in neurodegenerative disease. PLoS Biol. (2010) doi:10.1371/journal.pbio.1000291.
56. Baldo, B. et al. A screen for enhancers of clearance identifies huntingtin as a heat shock protein 90 (Hsp90) client protein. J. Biol. Chem. (2012) doi:10.1074/jbc.M111.294801.
57. Jackrel, M. E. & Shorter, J. Shock and awe: Unleashing the heat shock response to treat Huntington disease. Journal of Clinical Investigation (2011) doi:10.1172/JCI59190.
58. Scrivo, A., Bourdenx, M., Pampliega, O. & Cuervo, A. M. Selective autophagy as a potential therapeutic target for neurodegenerative disorders. The Lancet Neurology (2018) doi:10.1016/S1474-4422(18)30238-2.
59. Cuervo, A. M. & Wong, E. Chaperone-mediated autophagy: Roles in disease and aging. Cell Research (2014) doi:10.1038/cr.2013.153.
60. Boland, B. et al. Promoting the clearance of neurotoxic proteins in neurodegenerative disorders of ageing. Nature Reviews Drug Discovery (2018) doi:10.1038/nrd.2018.109.
61. Shibata, M. et al. Regulation of intracellular accumulation of mutant huntingtin by beclin 1. J. Biol. Chem. (2006) doi:10.1074/jbc.M600364200.
62. Wirawan, E. et al. Beclin 1: A role in membrane dynamics and beyond. Autophagy (2012) doi:10.4161/auto.8.1.16645.
63. Wu, J. C. et al. The regulation of N-terminal Huntingtin (Htt552) accumulation by Beclin1. Acta Pharmacol. Sin. (2012) doi:10.1038/aps.2012.14.
64. Ramaswamy, S., McBride, J. L. & Kordower, J. H. Animal models of Huntington's disease. ILAR Journal (2007) doi:10.1093/ilar.48.4.356.
65. Mangiarini, L. et al. Exon I of the HD gene with an expanded CAG repeat is sufficient to cause a progressive neurological phenotype in transgenic mice. Cell (1996) doi:10.1016/S0092-8674(00)81369-0.
66. Sathasivam, K. et al. Formation of polyglutamine inclusions in non-CNS tissue. Hum. Mol. Genet. (1999) doi:10.1093/hmg/8.5.813.
67. Watakabe, A. et al. Comparative analyses of adeno-associated viral vector serotypes 1, 2, 5, 8 and 9 in marmoset, mouse and macaque cerebral cortex. Neurosci. Res. (2015) doi:10.1016/j.neures.2014.09.002.
68. Li, J. Y., Popovic, N. & Brundin, P. The use of the R6 transgenic mouse models of Huntington' s disease in attempts to develop novel therapeutic strategies. NeuroRx (2005) doi:10.1602/neurorx.2.3.447.
69. Slow, E. J. et al. Selective striatal neuronal loss in a YAC128 mouse model of Huntington disease. Human Molecular Genetics (2003) doi:10.1093/hmg/ddg169.
70. Kim, J. Y., Grunke, S. D., Levites, Y., Golde, T. E. & Jankowsky, J. L. Intracerebroventricular viral injection of the neonatal mouse brain for persistent and widespread neuronal transduction. J. Vis. Exp. (2014) doi:10.3791/51863.
71. Jaeger, P. A. et al. Regulation of amyloid precursor protein processing by the beclin 1 complex. PLoS One (2010) doi:10.1371/journal.pone.0011102.
72. Gutekunst, C. A. Activating-Transcription-Factor-4 (ATF4)-Controlled Expression of

BECLIN1 to Reduce Huntingtin Aggregation in a Mouse Model of Huntington's Disease. (2020).